PHYSICAL REVIEW B VOLUME 4, NUMBER 3 1 AUGUST 1971

Spin-Wave Approach to Two-Magnon Raman Scattering in a Simple Antiferromagnet*

R. W. Davies, S. R. Chinn, and H. J. Zeiger
Lincoln Laboratory, Massachusetts Institute of Technology, Lexington, Massachusetts 02173
(Received 2 April 1971)

A spin-wave theory of two-magnon Raman scattering for a simple antiferromagnet at low temperatures is presented. The treatment is based on the Dyson-Maleev boson representation of the localized spin operators. At zero temperature, the theory yields results for the Raman cross section which are in excellent agreement with those which obtain from the Green's-function equation-of-motion method developed by Elliott and Thorpe. In the present theory, we derive an approximate cross-section formula in terms of renormalized one-magnon propagators and a vertex function which satisfies a general Bethe-Salpeter equation. Taking into consideration the lowest-order interaction processes, it is found that the experimentally observed shift of the Raman peak to lower energies with increasing temperature can satisfactorily be accounted for. However, it is also found that this lowest-order theory is inadequate for explaining the observed thermal broadening of the Raman spectra. The possibility that the observed broadening is due to damping of the one-magnon states is examined using a phenomenological width Γ for a zone-edge magnon. It is found that the necessary width is surprisingly large, although more accurate calculations of the damping of a zone-edge magnon are needed to eliminate this possibility. Higher-order irreducible vertex corrections in the two-magnon Bethe-Salpeter equation are also considered. An approximate cross-section formula which includes these higher-order corrections is obtained using a variational principle. The effect of these corrections on the Raman line shape has not yet been determined.

I. INTRODUCTION

Raman scattering of optical radiation by two-magnon excitations has been the subject of much recent experimental and theoretical study. Since the first observation of this effect in the antiferromagnets FeF_2 and MnF_2,[1] many other magnetic systems (such as $RbMnF_3$,[2] $KMnF_3$,[3] $KNiF_3$,[4] $CsMnF_3$,[5] NiF_2,[6] $RbNiF_3$[7,8]) have provided further experimental data on two-magnon Raman scattering. The first theoretical interpretation,[1,9] developed for zero-temperature and noninteracting magnons, was only qualitatively in agreement with the experimental results. This treatment was formulated with states composed of one magnon with wave vector $\vec{k}$, and another noninteracting magnon with wave vector $-\vec{k}$, combined to give a positive-parity state with $\vec{k}=0$, necessary for the Raman scattering process. Summing over all such combinations in the Brillouin zone predicted a spectral shape very similar to the two-magnon joint density of states. For the simple example of $RbMnF_3$ and other perovskite antiferromagnets, this led to a theoretical spectrum with a sharp discontinuity at twice the maximum zone-boundary magnon energy. Instead of this, actual spectra showed a very different line shape, with the peak occurring at slightly lower energy than predicted.

This discrepancy was removed by Elliott *et al.*,[10] and by Elliott and Thorpe,[11] who formulated the Green's-function theory for two-magnon scattering, and applied it at zero temperature. The main improvement in this theory was the explicit inclusion of the effects of magnon-magnon interactions which arise in the scattering process from the creation of magnons on adjacent spin sites. The simultaneous excitation of two adjacent spins leads to a net energy lower than if the spins were widely separated. If the spin system and Raman Hamiltonians are linearized in terms of magnon operators, this binding effect is neglected. The Green's-function decoupling scheme used by Elliott and Thorpe[11] explicitly included this effect of the magnon-magnon interaction. Their predictions were in excellent agreement with experiments, which showed asymmetric spectra having zero intensity at twice the maximum magnon energy, and largest intensity at an energy roughly one exchange constant lower.

However, up to the present, no theory has satisfactorily explained the behavior of the two-magnon spectra with increasing temperature. The experimental results are quite interesting. The common features in all cases are a decrease in energy of the position of the Raman peak with increasing temperature, and a broadening and disappearance of sharp features in the line shape. Even though the energy of the peak decreases, a nonzero Raman shift remains at the ordering temperature, and broad spectra persist up to several times T_N. The maximum energies in the spectra remain near their low-temperature values over the entire range of temperature. The qualitative explanation for this behavior lies in the proportionality of the Raman cross section to a spin pair-pair correlation function, which is a measure

of the short-range order persisting well above T_N, the temperature for long-range order.

The equation-of-motion method used by Elliott and Thorpe assumed a ground state for the spins and a decoupling scheme which were suitable only for $T = 0\,^\circ$K, and could not be readily extended to higher temperatures. A similar type of treatment has been given by Kawasaki,[12] with a random-phase approximation valid in the paramagnetic regime with $T > T_N$.

In as yet unpublished work, Sólyom[13] has treated the problem for low temperatures using the diagram technique developed by Vaks *et al.*[14] for treating spin-wave interactions in ferromagnets, and as extended to antiferromagnets by Pikalev *et al.*[15] Sólyom's theory takes into account the renormalization of the one-magnon energies with temperature in a self-consistent-field approximation, and also includes the temperature variation of the (renormalized) magnon occupation numbers, which would be expected to occur in the two-magnon Green's functions. At zero temperature his results are considerably more complicated than those of Elliott and Thorpe, but the difference appears to us quite minor, which ought to be the case considering the excellent agreement of the Elliott-Thorpe theory with the zero-temperature experimental results. As Sólyom points out, part of this difference is certainly due to the fact that his theory is based on the spin-wave ground state, whereas the simpler looking results given by Elliott and Thorpe are based on the Néel state. As has been discussed by these authors, this difference has little consequence in the two-magnon scattering problem.

Although Sólyom has computed no detailed spectra using his formulas, he has discussed the expected temperature dependence qualitatively. He concludes first that, due to the fact that the one-magnon renormalized energies decrease with temperature, the peak of the Raman spectrum must accordingly shift to lower energies, in agreement with the experimental results. Second, he concludes that the effect of the magnon occupation numbers $[2N(\bar{\Omega}_{\mathbf{f}}) + 1] = \coth(\beta\bar{\Omega}_{\mathbf{f}}/2)$, and of the Stokes factor $(1 - e^{-\beta\hbar\omega})^{-1}$ in the cross-section formula, should have the effect of making the contribution of low-energy magnons more and more important. This should lead to a broadening of the Raman peak with temperature, as observed experimentally. We believe that the first conclusion above is certainly valid. On the other hand, we believe that Sólyom's second conclusion is incorrect, and that the origin of the broadening of the Raman peak with increasing temperature is of a more complex nature than he suggests.

The present work, like Sólyom's, is directed at an attempt to understand the low-temperature features of two-magnon Raman spectra in a simple antiferromagnet. We also employ a graphical technique based, instead, on the Dyson-Maleev transformation, in the approximate form which has been discussed by Herbert.[16,17] We find, taking into account the renormalized one-magnon energies and the lowest-order interaction processes between the degenerate "up" and "down" magnons, a cross-section formula which appears to be quite similar to that given by Sólyom. However, calculations of the cross section from this formula indicate that, while the predicted peak of the Raman spectrum is in rather good agreement with the experimental results, the width of the resonance definitely is not. We find, in fact, that without damping, the width narrows slightly with increasing temperature, in contradiction with the conclusions of Sólyom. We conclude, therefore, that the origin of the observed broadening must be found in higher-order interaction processes (magnon lifetime effects, higher-order vertex corrections to the two-magnon Green's function, etc.) or perhaps in effects which cannot so easily be treated by the sort of spin-wave approach employed in this paper.

The effects of higher-order scattering processes are considered in the last part of this paper. Spectra are computed using a phenomenological width Γ for a zone-edge magnon, and Γ is chosen to give a broadening which is in rough agreement with the experimental results. It is found that the necessary Γ is surprisingly large—large compared to what we have been able to estimate through a rough evaluation of second-order self-energy graphs. However, to our knowledge, no really accurate calculations of the damping of a magnon at or near the zone edge in an antiferromagnet have yet been carried out. Harris *et al.*[18] have recently analyzed the damping of *long-wavelength* antiferromagnetic magnons in considerable detail, and here, as might be expected, the magnons are found to be long-lived well-defined excitations at sufficiently low temperatures. Unfortunately, the results of these authors are inappropriate for analyzing the problem considered here, because the damping of a magnon increases rapidly for shorter-wavelength magnons. Another possible source of broadening might arise from higher-order irreducible vertex corrections in the two-magnon Bethe-Salpeter equation. In this paper, we consider the second-order corrections formally. Roughly, these processes may be thought of as giving rise to a polarization interaction in analogy with the interacting Fermi gas. Although the cross section can no longer be evaluated exactly when these higher-order processes are included, we obtain an approximate formula using a variational principle. Numerical analysis of the re-

sulting cross-section formula is planned for a future publication.

Briefly, the organization of the remainder of the paper is as follows. In Sec. II we discuss the Hamiltonian and Raman cross-section formula using the Dyson-Maleev scheme, and state the various approximations we are making in the analysis. In Sec. III we present the general graphical interpretation of the resulting cross-section formula, in terms of renormalized magnon propagators, and a vertex function. In Sec. IV we evaluate the cross section using Hartree-Fock renormalized propagators and the lowest-order irreducible vertex interaction between the propagators. Spectra are computed as a function of temperature and compared with experimental results. As stated previously, the peak position of the spectra is found to be in rather good agreement with the experimental results, but the calculated linewidth is totally unsatisfactory. Section V is devoted to consideration of higher-order corrections. Lifetime effects are examined using a phenomenological width for a zone-edge magnon. In addition, an approximate cross-section formula which includes higher-order irreducible vertex corrections is obtained using a variational principle. Finally, Appendix A contains explicit expressions of various interaction matrix elements, and Appendix B gives a discussion of the variational principle for obtaining the Raman cross section.

II. HAMILTONIAN AND RAMAN CROSS SECTION

We consider an antiferromagnet consisting of two interpenetrating simple-cubic sublattices of a and b sites. We assume an isotropic Heisenberg exchange interaction between nearest neighbors only, and, with an infinitesimal anisotropy field to align the spins in the z direction, we take

$$\mathcal{H}=J\sum_{j\delta}\vec{S}_{j,a}\cdot\vec{S}_{j+\delta,b}\ , \tag{1}$$

where the sum over j is over the N sites of sublattice a, and the sum of δ is over the $z=6$ b sublattice nearest neighbors of the spin at site j,a. We apply the nonunitary Dyson-Maleev transformation to $\mathcal{H}$ in the form given by Herbert[16]:

$$\tilde{\mathcal{H}}=T\mathcal{H}T^{-1}\ ,$$

with the spin operators $\vec{S}$ going to $\tilde{\vec{S}}=T\vec{S}T^{-1}$. Then

$$\tilde{\mathcal{H}}=J\sum_{j\delta}\tilde{\vec{S}}_{j,a}\cdot\tilde{\vec{S}}_{j+\delta,b}\ , \tag{2}$$

and using the Holstein-Primakoff boson representation of the original $\tilde{S}$ operators, we obtain for the transformed $\tilde{S}$ operators

$$\tilde{S}^{+}_{j,a}=(2S)^{1/2}\left(1-\frac{a^{\dagger}_{j}a_{j}}{2S}\right)a_{j},\quad \tilde{S}^{+}_{j+\delta,b}=(2S)^{1/2}b^{\dagger}_{j+\delta}\ ,$$

$$\tilde{S}^{-}_{j,a}=(2S)^{1/2}a^{\dagger}_{j},\quad \tilde{S}^{-}_{j+\delta,b}=(2S)^{1/2}\left(1-\frac{b^{\dagger}_{j+\delta}b_{j+\delta}}{2S}\right)b_{j+\delta}\ ,$$

$$\tilde{S}^{z}_{j,a}=S-a^{\dagger}_{j}a_{j},\qquad \tilde{S}^{z}_{j+\delta,b}=-S+b^{\dagger}_{j+\delta}b_{j+\delta}\ . \tag{3}$$

We introduce Fourier transformations according to

$$a_{j}=\frac{1}{N^{1/2}}\sum_{\vec{k}}e^{-i\vec{k}\cdot\vec{X}_{j}}c_{\vec{k}}\ , \tag{4}$$

$$b_{j+\delta}=\frac{1}{N^{1/2}}\sum_{\vec{k}}e^{i\vec{k}\cdot\vec{X}_{j+\delta}}d^{\dagger}_{\vec{k}}\ , \tag{5}$$

and $\vec{X}_{j+\delta}=\vec{X}_{j}+\vec{\delta}$ with $\vec{\delta}$ a nearest-neighbor vector. In the usual manner, the part of the Hamiltonian involving products of two spin-wave operators is diagonalized by the Bogoliubov transformation

$$c_{\vec{k}}=u_{\vec{k}}\alpha_{\vec{k}}+v_{\vec{k}}\beta^{\dagger}_{\vec{k}}\ , \tag{6}$$

$$d_{\vec{k}}=u_{\vec{k}}\beta_{\vec{k}}+v_{\vec{k}}\alpha^{\dagger}_{\vec{k}}\ , \tag{7}$$

where the α's and β's satisfy the usual Bose commutation rules and $u^{2}_{\vec{k}}-v^{2}_{\vec{k}}=1$. The unperturbed part of the Hamiltonian is then found to be diagonalized for

$$u_{\vec{k}}=\left(\frac{1+[1-\gamma(\vec{k})^{2}]^{1/2}}{2[1-\gamma(\vec{k})^{2}]^{1/2}}\right)^{1/2}\ , \tag{8}$$

$$v_{\vec{k}}=-\left(\frac{1-[1-\gamma(\vec{k})^{2}]^{1/2}}{2[1-\gamma(\vec{k})^{2}]^{1/2}}\right)^{1/2}\ , \tag{9}$$

with

$$\gamma(\vec{k})=\gamma(-\vec{k})=\frac{1}{z}\sum_{\delta}e^{i\vec{k}\cdot\vec{\delta}} \tag{10}$$

or

$$\gamma(\vec{k})=\tfrac{1}{3}(\cos k_{x}a+\cos k_{y}a+\cos k_{z}a) \tag{11}$$

for the simple-cubic case. Other useful relations are

$$u^{2}_{\vec{k}}+v^{2}_{\vec{k}}=SJz/\Omega_{\vec{k}}\ , \tag{12}$$

$$u_{\vec{k}}v_{\vec{k}}=-\tfrac{1}{2}[\gamma(\vec{k})]\,SJz/\Omega_{\vec{k}}\ , \tag{13}$$

where

$$\Omega_{\vec{k}}=SJz[1-\gamma(\vec{k})^{2}]^{1/2}\ . \tag{14}$$

The higher-order terms in the Hamiltonian can now be expanded in terms of the α's, β's, u's, and v's. We treat these higher-order terms using the approximations discussed by Herbert,[17] and obtain

$$\tilde{\mathcal{H}}\simeq E_{0}+\mathcal{H}_{0}+V\ , \tag{15}$$

with

$$E_{0}=-NJzS(S+1)\ , \tag{16}$$

$$\mathcal{H}_{0}=\textstyle\sum_{\vec{k}}\Omega_{\vec{k}}(\alpha^{\dagger}_{\vec{k}}\alpha_{\vec{k}}+\beta^{\dagger}_{\vec{k}}\beta_{\vec{k}}+1)\ , \tag{17}$$

$$V=(-1)\frac{Jz}{N}\sum_{\vec{q}\vec{q}'\vec{p}\vec{p}'}\delta_{\vec{q}+\vec{p},\vec{q}'+\vec{p}'}(I^{\alpha\alpha}_{\vec{q}\vec{q}',\vec{p}\vec{p}'}\,\alpha^{\dagger}_{\vec{q}}\alpha^{\dagger}_{\vec{p}}\alpha_{\vec{p}'}\,\alpha_{\vec{q}'}$$

$$+I^{\beta\beta}_{\vec{q}\vec{q}',\vec{p}\vec{p}'}\beta^\dagger_{\vec{q}'}\beta^\dagger_{\vec{p}'}\beta_{\vec{p}}\beta_{\vec{q}}+I^{\alpha\beta}_{\vec{q}\vec{q}',\vec{p}\vec{p}'}\alpha^\dagger_{\vec{q}}\alpha_{\vec{q}'}\beta_{\vec{p}'}\beta_{\vec{p}}) \ . \quad (18)$$

In Eq. (18), the I's are complicated sums of products of the γ's, u's, and v's, and are given explicitly in Appendix A. Also in Appendix A we give the matrix elements which obtain using an alternative scheme[19] in which one applies the Dyson correspondence on sublattice a and the conjugate Dyson correspondence on sublattice b. (See Refs. 20 and 31 for further discussion of results using this alternative scheme.) Our form of V as given by Eq. (18) is slightly different from Herbert's form. This is due to a difference in the way we have introduced Fourier transforms [Eqs. (4) and (5)]. Our choice of Fourier transforms makes the analysis of the cross section quite analogous to electron-hole theory in the fermion problem.

Finally we list the approximations made to obtain V. First, we have ignored completely a three-body interaction term.[20] From the two-body-interaction terms we have ignored terms whose expectation value would vanish between any eigenstate of $\mathcal{H}_0$. We have also ignored small Oguchi[21] type of corrections to E_0 and $\mathcal{H}_0$ which arise in normal ordering the operators of V. Equation (18) also neglects umklapp processes, i.e., processes proportional to $\delta_{\vec{q}+\vec{p},\vec{q}'+\vec{p}'+\vec{K}}$ with $\vec{K}\neq 0$. In the subsequent analysis we shall also neglect the kinematic-interaction effect,[16,22] and perform traces in the usual unrestricted fashion. We replace the symbol $\tilde{\mathcal{H}}$ by $\mathcal{H}$ in the discussion which follows, treating it as one would an ordinary Hermitian Hamiltonian.

We take the two-magnon cross section to be proportional to

$$\bar{\mathcal{G}}(\hbar\omega)=\sum_{nm}\rho(E_n)|\langle m|M|n\rangle|^2 \times\delta(E_n-E_m+\hbar\omega) \ , \quad (19)$$

with $\omega=\omega_i-\omega_f$ the frequency shift of the scattered light and M a spin- and field-dependent operator discussed below. The kets $|n\rangle$ and $|m\rangle$ are eigenstates of $\mathcal{H}$, with

$$\mathcal{H}|n\rangle=E_n|n\rangle \quad \text{and} \quad \rho(\mathcal{H})|n\rangle=\rho(E_n)|n\rangle$$

and

$$\rho(\mathcal{H})=e^{-\beta\mathcal{H}}/\mathrm{Tr}\{e^{-\beta\mathcal{H}}\} \ .$$

$\bar{\mathcal{G}}(\hbar\omega)$ can then be computed using the standard temperature Green's-function method[23]:

$$\bar{\mathcal{G}}(\hbar\omega)=\frac{\mathrm{Im}\mathcal{G}(\hbar\omega+i0^+)}{\pi(1-e^{-\beta\hbar\omega})} \ , \quad (20)$$

with

$$\mathcal{G}(\hbar\omega+i0^+)=\mathcal{G}(\xi_l\to\hbar\omega+i0^+) \ , \quad (21)$$

$$\mathcal{G}(\xi_l)=\int_0^\beta e^{-\beta'\xi_l}\mathcal{G}(\beta',0)\,d\beta' \ , \quad (22)$$

$$\mathcal{G}(\beta',0)=\mathrm{Tr}\{\rho(\mathcal{H})T[M(\beta')M^\dagger(0)]\} \ , \quad (23)$$

and with $M(\beta')=e^{\beta'\mathcal{H}}Me^{-\beta'\mathcal{H}}$, and $\xi_l=2\pi il/\beta$. We also have the relation

$$\mathcal{G}(\beta',0)=\frac{1}{\beta}\sum_l e^{\beta'\xi_l}\mathcal{G}(\xi_l) \ , \quad (24)$$

with $\mathcal{G}(\xi_l)$ the Fourier coefficient in the expansion.

Following Elliott and Thorpe,[11] we take for the transition operator M of the two-magnon scattering process, the expression

$$M=\sum_{j\delta}\{B_1\vec{\epsilon}_i\cdot\vec{\epsilon}_f+B_3[\tfrac{1}{3}\vec{\epsilon}_i\cdot\vec{\epsilon}_f-\delta^{-2}(\vec{\delta}\cdot\vec{\epsilon}_i)(\vec{\delta}\cdot\vec{\epsilon}_f)]\} \times(\tilde{\vec{S}}_{j,a}\cdot\tilde{\vec{S}}_{j+\delta,b}) \ , \quad (25)$$

where $\vec{\epsilon}_i$ and $\vec{\epsilon}_f$ are the initial and final polarization vectors of the scattered light, and the sum is again over nearest-neighbor spin sites. The B_1 term gives rise to the Γ_1^+ scattering mode, the B_3 term gives rise to the Γ_3^+ mode. For nearest-neighbor interactions here and in the Hamiltonian $\mathcal{H}$, the B_1 term makes no contribution, because it is then proportional to the Hamiltonian, and the corresponding contribution to $M(\beta')$ is independent of β' (implying immediately that it makes no contribution to the cross section). Henceforth we drop the B_1 term.

In the present treatment we shall limit ourselves to considering terms in the product $M(\beta')M^\dagger(0)$ involving no more than four boson operators. In this approximation, the $\tilde{S}^z$ operators in M can be dropped. To see this, consider

$$\tilde{S}^z_{j,a}\tilde{S}^z_{j+\delta,b}=-S^2+S(a_j^\dagger a_j+b^\dagger_{j+\delta}b_{j+\delta})-a_j^\dagger a_j b^\dagger_{j+\delta}b_{j+\delta} \ . \quad (26)$$

The first two terms in Eq. (26) make no contribution to the Γ_3^+ mode because

$$\sum_{\vec{\delta}}\left[\frac{1}{3}\vec{\epsilon}_i\cdot\vec{\epsilon}_f-\frac{1}{\delta^2}(\vec{\delta}\cdot\vec{\epsilon}_i)(\vec{\delta}\cdot\vec{\epsilon}_f)\right]=0 \ .$$

It is then easy to see that the first nonvanishing contribution from the $\tilde{S}^z$ operators must involve products of at least six boson operators, which we neglect in the lowest-order spin-wave treatment. To the level at which we are working here, the entire contribution comes from the transverse ($\tilde{S}^\pm$) spin components, and we obtain

$$M\simeq SB_3\textstyle\sum_{\vec{k}}\phi(\vec{k})(c^\dagger_{\vec{k}}d^\dagger_{\vec{k}}+c_{\vec{k}}d_{\vec{k}}) \ , \quad (27)$$

with

$$\phi(\vec{k})=\phi(-\vec{k})=\sum_{\vec{\delta}}\left[\frac{1}{3}\vec{\epsilon}_i\cdot\vec{\epsilon}_f-\frac{1}{\delta^2}(\vec{\delta}\cdot\vec{\epsilon}_i)(\vec{\delta}\cdot\vec{\epsilon}_f)\right]e^{i\vec{k}\cdot\vec{\delta}} \ . \quad (28)$$

Then for $\mathcal{G}(\beta',0)$ we find

$$\mathcal{G}(\beta',0)\simeq S^2B_3^2\sum_{\vec{k}\vec{k}'}\phi(\vec{k})\phi(\vec{k}')\mathcal{G}_{\vec{k}\vec{k}'}(\beta',0) \ , \quad (29)$$

with

$$\mathcal{G}_{\vec{k}\vec{k}'}(\beta',0)=\mathrm{Tr}\{\rho(\mathcal{H})T[(c^\dagger_{\vec{k}}(\beta')d^\dagger_{\vec{k}'}(\beta')$$

$$+c_{\vec{k}'}(\beta')\,d_{\vec{k}'}(\beta'))(c_{\vec{k}}^{\dagger}d_{\vec{k}}^{\dagger}+c_{\vec{k}}\,d_{\vec{k}})]\}\ . \quad (30)$$

We next have to insert the Bogoliubov transformation [Eqs. (6) and (7)] into Eq. (30). Again we neglect terms which would give no contribution if we replaced $\mathcal{H}$ by $\mathcal{H}_0$. We then find the result

$$\mathcal{G}_{\vec{k}\vec{k}'}(\beta',0)\simeq(u_{\vec{k}}^2+v_{\vec{k}}^2)(u_{\vec{k}'}^2+v_{\vec{k}'}^2)\mathcal{G}_{\vec{k}\vec{k}'}^{(1)}(\beta',0)$$
$$+4u_{\vec{k}}v_{\vec{k}}u_{\vec{k}'}v_{\vec{k}'}[\mathcal{G}_{\vec{k}\vec{k}'}^{(2)}(\beta',0)+\mathcal{G}_{\vec{k}\vec{k}'}^{(3)}(\beta',0)]\ , \quad (31)$$

with

$$\mathcal{G}_{\vec{k}\vec{k}'}^{(1)}(\beta',0)=\mathrm{Tr}\{\rho(\mathcal{H})\,T[\alpha_{\vec{k}'}^{\dagger}(\beta')\,\beta_{\vec{k}'}^{\dagger}(\beta')\,\beta_{\vec{k}}\,\alpha_{\vec{k}}$$
$$+\alpha_{\vec{k}'}(\beta')\,\beta_{\vec{k}'}(\beta')\,\beta_{\vec{k}}^{\dagger}\,\alpha_{\vec{k}}^{\dagger}]\}\ , \quad (32)$$

$$\mathcal{G}_{\vec{k}\vec{k}'}^{(2)}(\beta',0)=\mathrm{Tr}\{\rho(\mathcal{H})\,T[\alpha_{\vec{k}'}^{\dagger}(\beta')\,\alpha_{\vec{k}'}(\beta')\,\alpha_{\vec{k}}^{\dagger}\,\alpha_{\vec{k}}$$
$$+\beta_{\vec{k}'}^{\dagger}(\beta')\,\beta_{\vec{k}'}(\beta')\,\beta_{\vec{k}}^{\dagger}\beta_{\vec{k}}]\}\ , \quad (33)$$

$$\mathcal{G}_{\vec{k}\vec{k}'}^{(3)}(\beta',0)=\mathrm{Tr}\{\rho(\mathcal{H})\,T[\alpha_{\vec{k}'}^{\dagger}(\beta')\,\alpha_{\vec{k}'}(\beta')\,\beta_{\vec{k}}^{\dagger}\beta_{\vec{k}}$$
$$+\beta_{\vec{k}'}^{\dagger}(\beta')\,\beta_{\vec{k}'}(\beta')\,\alpha_{\vec{k}}^{\dagger}\alpha_{\vec{k}}]\}\ . \quad (34)$$

We can now argue that it is an excellent approximation to ignore the terms involving $\mathcal{G}^{(2)}$ and $\mathcal{G}^{(3)}$. There are essentially two reasons for this. First, the relevant magnons involved in two-magnon scattering are those near the zone edge, and for zone-edge magnons $|u_{\vec{k}}v_{\vec{k}}|\ll(u_{\vec{k}}^2+v_{\vec{k}}^2)\simeq 1$. Second, and more importantly, the $\mathcal{G}^{(2)}$ and $\mathcal{G}^{(3)}$ Green's functions give no contribution to the noninteracting spectrum because the operators $\alpha_{\vec{k}}^{\dagger}\alpha_{\vec{k}}$ and $\beta_{\vec{k}}^{\dagger}\beta_{\vec{k}}$ commute with $\mathcal{H}_0$, making these Green's functions independent of β'. Likewise one can see that the simplest class of higher-order corrections to these Green's functions can be ignored for the same reason.

With the above approximation, the cross section may be obtained from

$$\mathcal{G}(\xi_l)=S^2B_3^2\sum_{\vec{k}\vec{k}'}\phi(\vec{k})\,\phi(\vec{k}')\,(u_{\vec{k}}^2+v_{\vec{k}}^2)\,(u_{\vec{k}'}^2+v_{\vec{k}'}^2)$$
$$\times[\mathcal{S}_{\vec{k}\vec{k}'}(\xi_l)+\mathcal{S}_{\vec{k}\vec{k}'}(-\xi_l)]\ , \quad (35)$$

where

$$\mathcal{S}_{\vec{k}\vec{k}'}(\beta',0)=\mathrm{Tr}\{\rho(\mathcal{H})T[\alpha_{\vec{k}'}^{\dagger}(\beta')\,\beta_{\vec{k}'}^{\dagger}(\beta')\,\beta_{\vec{k}}\,\alpha_{\vec{k}}]\} \quad (36)$$

and

$$\mathcal{S}_{\vec{k}\vec{k}'}(\beta',0)=\frac{1}{\beta}\sum_l e^{\beta'\xi_l}\,\mathcal{S}_{\vec{k}\vec{k}'}(\xi_l)\ . \quad (37)$$

Finally, using the cubic symmetry of the system, Eq. (35) may be rewritten

$$\mathcal{G}(\xi_l)=\tfrac{4}{3}g(\vec{\epsilon}_i,\vec{\epsilon}_f)NS^2B_3^2\frac{1}{N}\sum_{\vec{k}\vec{k}'}f(\vec{k})f(\vec{k}')$$
$$\times(u_{\vec{k}}^2+v_{\vec{k}}^2)(u_{\vec{k}'}^2+v_{\vec{k}'}^2)[\mathcal{S}_{\vec{k}\vec{k}'}(\xi_l)+\mathcal{S}_{\vec{k}\vec{k}'}(-\xi_l)]\ , \quad (38)$$

where $f(\vec{k})=(\cos k_x a-\cos k_y a)$ is the symmetrization factor for the Γ_3^+ mode, and

$$g(\vec{\epsilon}_i,\vec{\epsilon}_f)=[(\epsilon_i^x\epsilon_f^x)^2+(\epsilon_i^y\epsilon_f^y)^2+(\epsilon_i^z\epsilon_f^z)^2$$
$$-\epsilon_i^x\epsilon_f^x\epsilon_i^y\epsilon_f^y-\epsilon_i^x\epsilon_f^x\epsilon_i^z\epsilon_f^z-\epsilon_i^y\epsilon_f^y\epsilon_i^z\epsilon_f^z] \quad (39)$$

gives the characteristic polarization dependence of the Γ_3^+ mode.

III. GENERAL GRAPHICAL ANALYSIS

The quantity $\mathcal{S}_{\vec{k}\vec{k}'}(\xi_l)$ can now be analyzed by standard[23] graphical techniques, in terms of the sum of all linked (or connected) "polarization" graphs. First we define the basic unperturbed propagators

$$D_{\vec{k}\alpha}^{(0)}(\beta_i,\beta_j)=\mathrm{Tr}\{\rho(\mathcal{H}_0)T[\alpha_{\vec{k}}^{\dagger}(\beta_i)\,\alpha_{\vec{k}}(\beta_j)]\}\ , \quad (40)$$

$$D_{\vec{k}\beta}^{(0)}(\beta_i,\beta_j)=\mathrm{Tr}\{\rho(\mathcal{H}_0)\,T[\beta_{\vec{k}}^{\dagger}(\beta_i)\beta_{\vec{k}}(\beta_j)]\}\ , \quad (41)$$

with $\mathcal{O}(\beta_i)=e^{\beta_i\mathcal{H}_0}\,\mathcal{O}\,e^{-\beta_i\mathcal{H}_0}$. We denote $D_{\vec{k}\alpha}^{(0)}$ by a single solid line with one arrow, going *from* β_i *to* β_j. We denote $D_{\vec{k}\beta}^{(0)}$ by a single solid line with two arrows, going *from* β_j *to* β_i. We introduce Fourier representations according to

$$D_{\vec{k}\alpha}^{(0)}(\beta_i,\beta_j)=\frac{1}{\beta}\sum_l e^{\xi_l(\beta_i-\beta_j)}\,D_{\vec{k}\alpha}^{(0)}(\xi_l)\ , \quad (42)$$

$$D_{\vec{k}\beta}^{(0)}(\beta_i,\beta_j)=\frac{1}{\beta}\sum_l e^{\xi_l(\beta_j-\beta_i)}\,D_{\vec{k}\beta}^{(0)}(\xi_l)\ , \quad (43)$$

and find

$$D_{\vec{k}\alpha}^{(0)}(\xi_l)=(\Omega_{\vec{k}}-\xi_l)^{-1}\ , \quad (44)$$

$$D_{\vec{k}\beta}^{(0)}(\xi_l)=(\Omega_{\vec{k}}+\xi_l)^{-1}\ . \quad (45)$$

The corrected propagators are obtained from Eqs. (40) and (41) by replacing $\mathcal{H}_0$ by $\mathcal{H}$ everywhere. From Dyson's equation, we will obtain

$$D_{\vec{k}\alpha}(\xi_l)=[\Omega_{\vec{k}}-\xi_l-G_{\vec{k}\alpha}(\xi_l)]^{-1}\ , \quad (46)$$

$$D_{\vec{k}\beta}(\xi_l)=[\Omega_{\vec{k}}+\xi_l-G_{\vec{k}\beta}(\xi_l)]^{-1}\ , \quad (47)$$

where the G's are the self-energy functions, $G_{\vec{k}\beta}(\xi_l)=G_{\vec{k}\alpha}(-\xi_l)$ and $D_{\vec{k}\beta}(\xi_l)=D_{\vec{k}\alpha}(-\xi_l)$ from mode degeneracy. We represent the corrected propagators using double solid lines in place of single solid lines.

The general graphical representation of $\mathcal{S}_{\vec{k}\vec{k}'}(\xi_l)$ is shown in Fig. 1 in terms of the corrected magnon propagators, and a vertex function $\Lambda_{\vec{k}\vec{k}'}(\xi_l,\xi_{l_1})$. We then have, explicitly

$$\mathcal{S}_{\vec{k}\vec{k}'}(\xi_l)=\frac{1}{\beta}\sum_{l_1}D_{\vec{k}\alpha}(\xi_l+\xi_{l_1})\,D_{\vec{k}\beta}(\xi_{l_1})\,\Lambda_{\vec{k}\vec{k}'}(\xi_l,\xi_{l_1})\ . \quad (48)$$

The vertex function in Eq. (48) satisfies a Bethe-Salpeter equation of the form

$$\Lambda_{\vec{k}\vec{k}'}(\xi_l,\xi_{l_1})=\delta_{\vec{k},\vec{k}'}+\frac{Jz}{N\beta}\sum_{\vec{k}_1}\sum_{l_2}\tilde{I}_{\vec{k}\vec{k}_1,\vec{k}_1\vec{k}}^{\alpha\beta}(\xi_{l_1},\xi_{l_2})$$
$$\times D_{\vec{k}_1\alpha}(\xi_l+\xi_{l_2})\,D_{\vec{k}_1\beta}(\xi_{l_2})\,\Lambda_{\vec{k}_1\vec{k}'}(\xi_l,\xi_{l_2})\ , \quad (49)$$

where $\tilde{I}^{\alpha\beta}$ is the sum of all the irreducible interaction parts. Let us next write

$$\mathcal{G}(\xi_l)=\mathcal{G}^{(+)}(\xi_l)+\mathcal{G}^{(+)}(-\xi_l)\ , \quad (50)$$

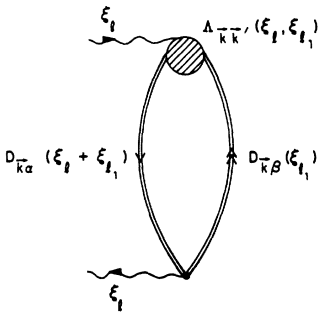

FIG. 1. Graphical representation of the scattering function $\mathcal{S}_{\vec{k}\vec{k}'}(\xi_l)$ with corrected magnon propagators.

where from Eq. (38)

$$\mathcal{G}^{(+)}(\xi_l) = \tfrac{4}{3} g(\vec{\epsilon}_i, \vec{\epsilon}_f) NS^2 B_3^2 \times \frac{1}{N} \sum_{\vec{k}\vec{k}'} f(\vec{k}) f(\vec{k}') (u_{\vec{k}}^2 + v_{\vec{k}}^2)(u_{\vec{k}'}^2 + v_{\vec{k}'}^2) \mathcal{S}_{\vec{k}\vec{k}'}(\xi_l) \ . \quad (51)$$

Combining Eqs. (48) and (51), we obtain

$$\mathcal{G}^{(+)}(\xi_l) = \tfrac{4}{3} g(\vec{\epsilon}_i, \vec{\epsilon}_f) NS^2 B_3^2 \frac{1}{N\beta} \sum_{\vec{k}} \sum_{l_1} f(\vec{k})(u_{\vec{k}}^2 + v_{\vec{k}}^2) \times D_{\vec{k}\alpha}(\xi_l + \xi_{l_1}) D_{\vec{k}\beta}(\xi_{l_1}) \Lambda_{\vec{k}}(\xi_l, \xi_{l_1}) \ , \quad (52)$$

where we have defined

$$\Lambda_{\vec{k}}(\xi_l, \xi_{l_1}) = \sum_{\vec{k}'} f(\vec{k}') (u_{\vec{k}'}^2 + v_{\vec{k}'}^2) \Lambda_{\vec{k}\vec{k}'}(\xi_l, \xi_{l_1}) \ . \quad (53)$$

From Eqs. (49) and (53), the new vertex function satisfies

$$\Lambda_{\vec{k}}(\xi_l, \xi_{l_1}) = f(\vec{k})(u_{\vec{k}}^2 + v_{\vec{k}}^2) + \frac{Jz}{N\beta} \sum_{\vec{k}_1} \sum_{l_2} I^{\alpha\beta}_{\vec{k}\vec{k}_1, \vec{k}_1\vec{k}}(\xi_{l_1}, \xi_{l_2}) \times D_{\vec{k}_1\alpha}(\xi_l + \xi_{l_2}) D_{\vec{k}_1\beta}(\xi_{l_2}) \Lambda_{\vec{k}_1}(\xi_l, \xi_{l_2}) \ . \quad (54)$$

Equations (20), (21), (50), (52), and (54) are the general equations of the present theory.

IV. LOWEST-ORDER PROCESSES

The simplest self-energy processes to take into account arise from the first-order skeleton self-energy graphs. In analogy with the fermion problem, we shall refer to these as Hartree-Fock graphs (called "cactus" graphs in the paper of Herbert[17]). Typical Hartree-Fock graphs are shown in Fig. 2. As discussed by Herbert, the solution of the Hartree-Fock equation yields renormalized energies $\overline{\Omega}_{\vec{k}}$ given by

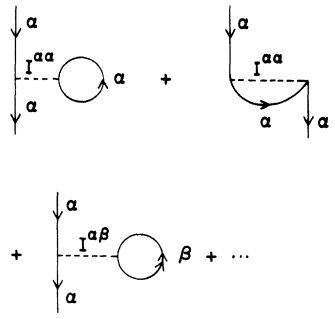

FIG. 2. Typical Hartree-Fock graphs for a renormalizing one-magnon propagators $D_{\vec{k}\alpha}(\xi_l)$.

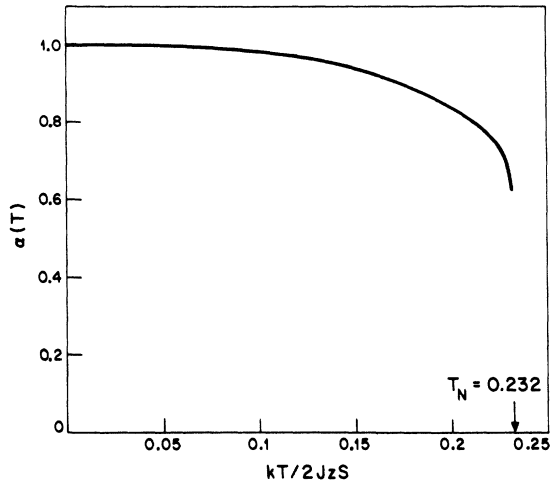

FIG. 3. One-magnon energy renormalization factor $\alpha(T)$ as a function of normalized temperature, $kT/2JzS$.

$$\overline{\Omega}_{\vec{k}} = \Omega_{\vec{k}}\, \alpha(T) \ , \quad (55)$$

where $\alpha(T)$ depends only on temperature and is given by the implicit equation

$$\alpha(T) = 1 - \frac{1}{JzS^2} \frac{1}{N} \sum_{\vec{q}} \Omega_{\vec{q}} (e^{\beta \Omega_{\vec{q}} \alpha(T)} - 1)^{-1} \ . \quad (56)$$

This same result (but including a small Oguchi correction which is finite at $T = 0\,^\circ\mathrm{K}$) was first obtained by Bloch[24, 25] from a variational calculation, and has been obtained in various ways by others.[26] A plot of $\alpha(T)$ for $S = 1$ is shown in Fig. 3 (we have plotted only the upper physical root). In this, and all numerical calculations to follow, we take the case of a cubic structure with $z = 6$, $S = 1$, corresponding to the example of $KNiF_3$. There is no solution of Eq. (56) beyond a maximum temperature which is within a few percent of various theoretical determinations[27, 28] of the Néel ordering temperature T_N.

If we now compute $\mathcal{G}^{(+)}(\xi_l)$ ignoring interactions other than the Hartree-Fock renormalization of the energies, we easily obtain [with $\Lambda_{\vec{k}}(\xi_l, \xi_{l_1}) = f(\vec{k}) \times (u_{\vec{k}}^2 + v_{\vec{k}}^2)$ in this approximation]

$$\mathcal{G}^{(+)}(\xi_l) = \tfrac{4}{3} g(\vec{\epsilon}_i, \vec{\epsilon}_f) NS^2 B_3^2 \times \frac{1}{N} \sum_{\vec{k}} f(\vec{k})^2 (u_{\vec{k}}^2 + v_{\vec{k}}^2)^2 \frac{2N(\overline{\Omega}_{\vec{k}}) + 1}{2\overline{\Omega}_{\vec{k}} - \xi_l} \ , \quad (57)$$

so that

$$\bar{\mathcal{G}}(\hbar\omega) = \frac{4}{3\pi} g(\vec{\epsilon}_i, \vec{\epsilon}_f) NS^2 B_3^2 (1 - e^{-\beta\hbar\omega})^{-1} \times \mathrm{Im} \frac{1}{N} \sum_{\vec{k}} f(\vec{k})^2 \left(\frac{SJz}{\Omega_{\vec{k}}}\right)^2 \times [2N(\bar{\Omega}_{\vec{k}}) + 1] \frac{4\bar{\Omega}_{\vec{k}}}{4\bar{\Omega}_{\vec{k}}^2 - (\hbar\omega + i0^+)^2} \quad . \quad (58)$$

In the equation above, $N(\bar{\Omega}_{\vec{k}})$ denotes the Bose function. This result is essentially identical to the noninteracting result obtained by Sólyom,[13] except that the over-all amplitude factor S^2 in our theory is renormalized with temperature (decreased) in his theory. This difference may be due to our complete neglect of higher-order terms in the Raman cross-section formula. The difference is important as far as the temperature variation of the Raman amplitude is concerned, but it plays no role in the shape of the spectrum. The same remark applies to the interacting spectra in the two theories. We shall discuss the temperature dependence of the Raman amplitude in more detail in Sec. V.

Next we consider the lowest-order vertex corrections to the interacting-magnon spectrum. In this approximation the vertex function satisfies the simple "ladder" approximation Bethe-Salpeter equation. In this approximation we have (see Appendix A for the explicit expressions for various matrix elements)

$$\tilde{I}^{\alpha\beta}_{\vec{k}\vec{k}_1,\vec{k}_1\vec{k}}(\xi_{l_1}, \xi_{l_2}) = I^{\alpha\beta}_{\vec{k}\vec{k}_1,\vec{k}_1\vec{k}} = \{\tfrac{1}{2}\gamma(\vec{k} - \vec{k}_1)[(u_{\vec{k}}^2 + v_{\vec{k}}^2)(u_{\vec{k}_1}^2 + v_{\vec{k}_1}^2) + 1] - \tfrac{1}{2}\gamma(\vec{k})\gamma(\vec{k}_1)[(u_{\vec{k}}^2 + v_{\vec{k}}^2)(u_{\vec{k}_1}^2 + v_{\vec{k}_1}^2) + (u_{\vec{k}}^2 + v_{\vec{k}}^2) - (u_{\vec{k}_1}^2 + v_{\vec{k}_1}^2)]\} \quad . \quad (59)$$

We use the relations

$$\sum_{\vec{k}} f(\vec{k})\gamma(\vec{k})g(\vec{k}) = 0 \quad , \quad (60)$$

$$\sum f(\vec{k})\gamma(\vec{k} - \vec{k}_1)g(\vec{k}) = \frac{f(\vec{k}_1)}{z} \sum_{\vec{k}} f(\vec{k})^2 g(\vec{k}) \quad , \quad (61)$$

where $g(\vec{k})$ has cubic symmetry. From Eqs. (52), (54), and (59) an exact solution for $\mathcal{G}^{(+)}(\xi_l)$ is then found:

$$\mathcal{G}^{(+)}(\xi_l) = \tfrac{1}{3} g(\vec{\epsilon}_i, \vec{\epsilon}_f) NS^2 B_3^2 \times \left[\frac{L^{(2)} + \frac{1}{2}J(L^{(1)}L^{(1)} - L^{(2)}L^{(0)})}{1 - \frac{1}{2}J(L^{(0)} + L^{(2)}) - \frac{1}{4}J^2(L^{(1)}L^{(1)} - L^{(2)}L^{(0)})}\right] \quad , \quad (62)$$

with

$$L^{(m)}(\xi_l) = \frac{1}{N\beta} \sum_{\vec{k}} \sum_{l_1} f(\vec{k})^2 (u_{\vec{k}}^2 + v_{\vec{k}}^2)^m D_{\vec{k}\alpha}(\xi_l + \xi_{l_1}) D_{\vec{k}\beta}(\xi_{l_1}) \quad (63)$$

or

$$L^{(m)}(\xi_l) = \frac{1}{N} \sum_{\vec{k}} f(\vec{k})^2 (u_{\vec{k}}^2 + v_{\vec{k}}^2)^m \frac{2N(\bar{\Omega}_{\vec{k}}) + 1}{2\bar{\Omega}_{\vec{k}} - \xi_l} \quad (64)$$

for the case where we use Hartree-Fock propagators for the D's. We remark that the $\mathcal{G}^{(+)}(-\xi_l)$ term in the cross-section expression can be neglected for the Stokes ($\omega > 0$) scattering, because it contains no imaginary part to the level of the Hartree-Fock approximation. Even if we were to use propagators which contained some damping, the contribution of the $\mathcal{G}^{(+)}(-\xi_l)$ component to the Stokes cross section should be extremely small, since it involves no resonant denominators.

Both our interacting cross-section formula [Eq. (62)] and the one obtained by Sólyom[13] are somewhat complicated and hard to compare precisely. However, neglecting nonresonant contributions in both theories, and also approximating the factors $(U_{\vec{k}}^2 + v_{\vec{k}}^2)^m = (SJz/\Omega_{\vec{k}})^m \simeq 1$, both theories reduce to give an interacting Stokes cross section proportional to $\mathrm{Im}\{L^{(0)}(\xi_l)/[1 - JL^{(0)}(\xi_l)]\}$. Thus we believe that the content of the two theories is nearly identical. Furthermore, we find that our cross-section expression is very insensitive to the approximation $L^{(0)} \simeq L^{(1)} \simeq L^{(2)}$. The reason is that the density-of-states function is so strongly peaked near the zone edge. This, incidently, appears to be the reason that Sólyom's qualitative conclusions, concerning the broadening of the Raman peak, fail. Also we can state rigorously that both theories yield no Raman intensity beyond the Hartree-Fock maximum ($2\bar{\Omega}_m$), because the Green's functions contain no imaginary part above this energy. This result is *not* in accordance with the experimental observations.

In Fig. 4 we show a series of Raman spectra for various temperatures computed using Eqs. (62) and (64). The calculations were carried out by first rewriting Eq. (64) in the equivalent form (as $2\Gamma \to 0^+$)

$$L^{(m)}(\hbar\omega) = \frac{2}{\pi} \int_0^{2\Omega_{\max}} E'\,dE' \left(\frac{2\Omega_{\max}}{E'}\right)^m \frac{2N(\frac{1}{2}\alpha E') + 1}{\alpha E' - \hbar\omega - i2\Gamma} \times \mathrm{Im} \frac{1}{N} \sum_{\vec{k}} \frac{f(\vec{k})^2}{E'^2 - 4\Omega_{\vec{k}}^2 - i0^+} \quad , \quad (65)$$

where $\Omega_{\max} = SJz$, $\alpha = \alpha(T)$ is the energy renormalization factor, and 2Γ is chosen to be a suitably small number. The $\vec{k}$ summation in Eq. (65) can be evaluated using the standard transformation to Bessel functions. The remaining E' integration was then performed numerically on a computer, with 2Γ chosen to be as small as practically possible for such a numerical integration, and small enough to ensure that the results were independent of Γ for the limiting case of $\Gamma \to 0$. It is worth noting also that the amplitude of our computed

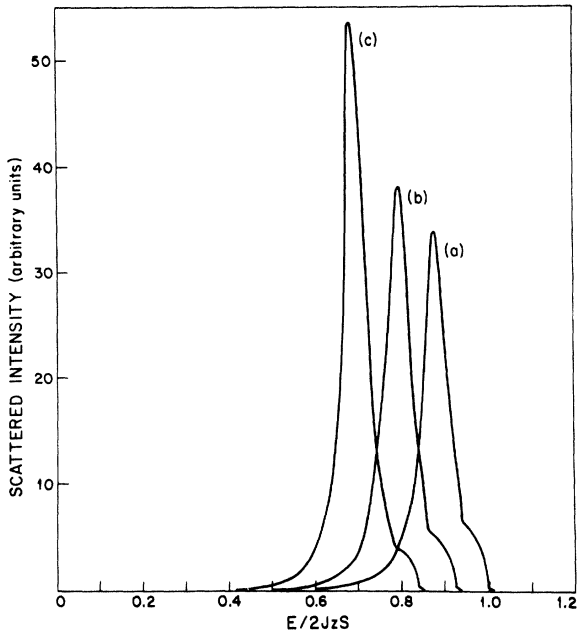

FIG. 4. Theoretical two-magnon Raman spectra for various temperatures as a function of normalized energy, $E/2JzS$, with $2\Gamma/2JzS = 0.0009$. Curve (a) $T = 0$, curve (b) $T = 0.69T_N$, curve (c) $T = 0.86T_N$, where $kT_N = 0.232 \times (2JzS)$, as found from $\alpha(T)$.

spectrum for $T = 0\,^{\circ}\mathrm{K}$ is in excellent agreement with the results found from the Elliott-Thorpe formulation.

From Fig. 4, we see that while the Raman peak correctly shifts toward lower energies with increasing temperature, the linewidth slightly narrows, in strong disagreement with the experimental results. In Fig. 5 we compare the experimental results for the peak position as a function of temperature, for the antiferromagnet $KNiF_3$ ($S = 1$), with the theoretical peak predicted by the equations presented in this section. The agreement is seen to be satisfactory.

V. HIGHER-ORDER PROCESSES

Figure 6 shows a plot of the measured Raman linewidth for $KNiF_3$ as a function of temperature. A natural first question to investigate is whether this broadening can be ascribed to damping of the one-magnon states, which arises in lowest order from the imaginary part of the self-energy in diagrams of the type shown in Fig. 7. The contribution to $\Gamma_{\vec{k}} = \mathrm{Im}G_{\vec{k}\alpha}(\bar{\Omega}_{\vec{k}} + i0^+)$ from the second-order diagrams of Fig. 7 is given by

$$\Gamma_{\vec{k}} = \pi(1 - e^{-\beta\bar{\Omega}_{\vec{k}}}) \times \frac{(Jz)^2}{N^2} \sum_{\vec{k}'\vec{q}} M(\vec{k},\vec{k}',\vec{q})\,[N(\bar{\Omega}_{\vec{k}-\vec{q}}) + 1]\,[N(\bar{\Omega}_{\vec{k}'-\vec{q}}) + 1] \times N(\bar{\Omega}_{\vec{k}'})\,\delta(\bar{\Omega}_{\vec{k}-\vec{q}} + \bar{\Omega}_{\vec{k}'-\vec{q}} - \bar{\Omega}_{\vec{k}'} - \bar{\Omega}_{\vec{k}}) , \quad (66)$$

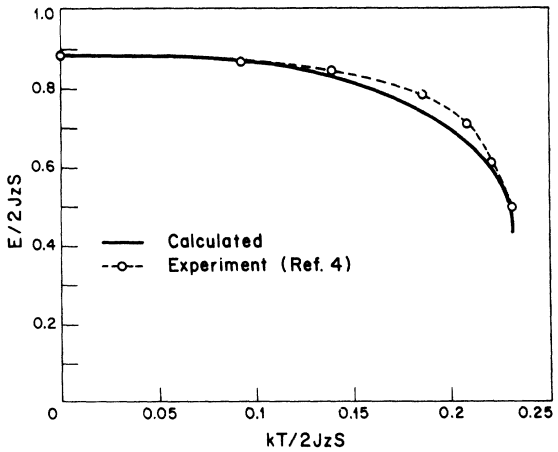

FIG. 5. Experimental and theoretical Raman peak positions as a function of temperature for $KNiF_3$. The temperatures for the experimental curve have been normalized to make the theoretical and experimental Néel temperatures coincide.

with

$$M(\vec{k},\vec{k}',\vec{q}) = I^{\alpha\beta}_{(\vec{k}-\vec{q})\vec{k},\,\vec{k}'(\vec{k}'-\vec{q})}\, I^{\alpha\beta}_{\vec{k}(\vec{k}-\vec{q}),(\vec{k}'-\vec{q})\vec{k}'} + \left(I^{\alpha\alpha}_{(\vec{k}-\vec{q})\vec{k},(-\vec{k}'+\vec{q})(-\vec{k}')} + I^{\alpha\alpha}_{(-\vec{k}'+\vec{q})(-\vec{k}'),(\vec{k}-\vec{q})\vec{k}}\right) \times \left(I^{\alpha\alpha}_{\vec{k}(\vec{k}-\vec{q}),(-\vec{k}')(-\vec{k}'+\vec{q})} + I^{\alpha\alpha}_{(-\vec{k}')(-\vec{k}'+\vec{q}),\vec{k}(\vec{k}-\vec{q})} + I^{\alpha\alpha}_{\vec{k}(-\vec{k}'+\vec{q}),(-\vec{k}')(\vec{k}-\vec{q})} + I^{\alpha\alpha}_{(-\vec{k}')(\vec{k}-\vec{q}),\vec{k}(-\vec{k}'+\vec{q})}\right) . \quad (67)$$

In writing down the above results, we have used Hartree-Fock propagators in place of the bare propagators. An expression quite similar to Eq. (66) has been obtained by Harris *et al.*,[18] and these authors have analyzed in detail the damping of long-wavelength magnons.

In order to investigate the question of damping in a qualitative way, we have done the following

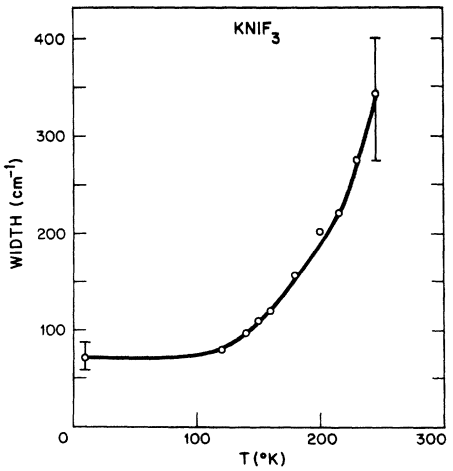

FIG. 6. Measured two-magnon Raman linewidth (full width, half-maximum) for $KNiF_3$ (from Ref. 4).

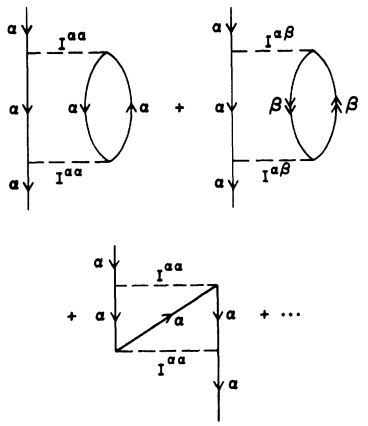

FIG. 7. Typical second-order diagrams contributing to the imaginary part of the one-magnon self-energy.

calculation. To a rough first approximation, the effect of the damping of the one-magnon states will be to replace the quantity 2Γ (where formerly $2\Gamma \to 0$) in Eq. (65) by $2\Gamma_{\vec{k}} = 2\,\mathrm{Im}G_{\vec{k}\alpha}$, for $\vec{k}$ corresponding to a near-zone-edge magnon. Figure 8 shows a set of two-magnon spectra computed from Eqs. (62) and (65) using values for Γ which yield widths in rough agreement with the measured experimental widths. The shapes of the computed spectra are also in qualitative agreement with the experimental shapes, except that the computed spectra appear to have rather too much tail away from the resonance. The values of Γ for the three curves (a), (b), and (c) of Fig. 8 are $\Gamma/SJz = 0.0009$, 0.05, 0.105, respectively. These latter two values are at least one order of magnitude larger than what we have been able to estimate through a crude calculation of $\Gamma_{\vec{k}}$ from the second-order self-energy graphs. However, the calculation of $\Gamma_{\vec{k}}$ for a zone-edge magnon is complicated. Among other approximations, our calculations were done using a spherical model for the energy surfaces, with energies which are taken to be linear functions of $|\vec{k}|$. Obviously, better calculations of $\Gamma_{\vec{k}}$ are needed before the damping of one-magnon states can be ruled out as an important contribution to the broadening of the Raman spectra. It should be noted that for the Γ values given above, the zone-edge magnons are still well-defined excitations in the sense that $\Gamma/SJz \ll 1$. Also we remark that it is clear in going beyond the Hartree-Fock approximation that the self-energy renormalization is $\vec{k}$ dependent, i.e., long- and short-wavelength magnons may, perhaps, renormalize in quite different ways. This could also contribute to broadening.

TABLE I. Comparison of theoretical and experimental two-magnon peak amplitudes.

Temperature	α^2	Normalized theoretical amplitude (from Fig. 8)	Normalized experimental amplitude
0	1.00	1.00	1.00
$0.69T_N$	0.86	0.44	0.55 ± 0.10
$0.86T_N$	0.71	0.31	0.34 ± 0.07

Finally, it is interesting to compare the experimental temperature dependence of the Raman peak amplitude with the amplitudes, shown in Fig. 8, obtained using the phenomenological damping of one-magnon states. The experimental determination of the amplitude is somewhat more difficult than that of the line position or width, since there is no temperature-independent reference feature in the spectrum and the sample absorption is changing slightly with temperature. However, using a rough correction to allow for the measured absorption, we present in Table I a comparison of the peak amplitudes of Fig. 8 with the experimental values. We also give the value of α^2 corresponding to the temperature-dependent amplitude renormalization factor of Sólyom. Without damping (see Fig. 4), this factor is approximately sufficient to offset the increase in amplitude due to the Stokes and Bose temperature factors, and this would yield an amplitude which is roughly constant. To the level we have carried the present theory, Sólyom's amplitude renormalization factor does not appear to enter. However, ignoring this factor completely, Table I shows that phenomenological damping yields, perhaps only fortuitously, an amplitude dependence in reasonable agreement with the experimental results.

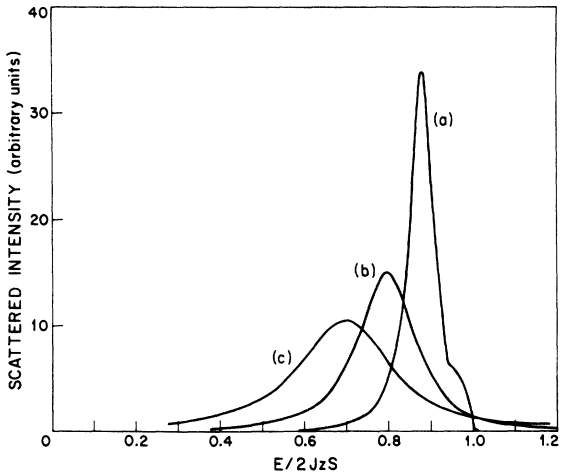

FIG. 8. Computed two-magnon Raman spectra as a function of normalized energy $E/2JzS$, using phenomenological magnon lifetimes necessary to fit the experimental data (Fig. 6). (a) $T=0$, $\Gamma/JzS=0.0009$; (b) $T=0.69T_N$, $\Gamma/JzS=0.05$; (c) $T=0.86T_N$, $\Gamma/JzS=0.105$.

Another possible source of broadening of the two-magnon Raman spectra might arise from higher-order irreducible vertex corrections in the two-magnon Bethe-Salpeter equation. Typical second-order corrections are shown in Fig. 9. These diagrams can roughly be thought of as polarization processes which give rise to a modified interaction between the primary α and β Raman scattering magnons. Using Hartree-Fock propagators to evaluate these diagrams, we find that $\tilde{I}^{\alpha\beta}$ in the Bethe-Salpeter equation [Eq. (54)] is given by

$$\tilde{I}^{\alpha\beta}_{\vec{k}\vec{k}_1,\vec{k}_1\vec{k}}(\xi_{l_1},\xi_{l_2}) = I^{\alpha\beta}_{\vec{k}\vec{k}_1,\vec{k}_1\vec{k}} + K_{\vec{k}\vec{k}_1}(\xi_{l_1},\xi_{l_2}) , \tag{68}$$

where K essentially plays the role of a "dielectric constant," and is given by

$$K_{\vec{k}\vec{k}_1}(\xi_{l_1},\xi_{l_2}) = \frac{Jz}{N}\sum_{\vec{k}'} \left(I^{\alpha\alpha}_{\vec{k}\vec{k}_1,(\vec{k}_1-\vec{k}+\vec{k}')\vec{k}'} + I^{\alpha\alpha}_{(\vec{k}_1-\vec{k}+\vec{k}')\vec{k}',\vec{k}\vec{k}_1} + I^{\alpha\alpha}_{(\vec{k}_1-\vec{k}+\vec{k}')\vec{k}_1,\vec{k}\vec{k}'} + I^{\alpha\alpha}_{\vec{k}\vec{k}',(\vec{k}_1-\vec{k}+\vec{k}')\vec{k}_1}\right)$$

$$\times I^{\alpha\beta}_{\vec{k}',(\vec{k}_1-\vec{k}+\vec{k}'),\vec{k}_1\vec{k}}[N(\bar{\Omega}_{\vec{k}'}) - N(\bar{\Omega}_{\vec{k}_1-\vec{k}+\vec{k}'})]\frac{2(\bar{\Omega}_{\vec{k}_1-\vec{k}+\vec{k}'} - \bar{\Omega}_{\vec{k}'})}{(\bar{\Omega}_{\vec{k}_1-\vec{k}+\vec{k}'} - \bar{\Omega}_{\vec{k}'})^2 - (\xi_{l_1}-\xi_{l_2})^2} + \frac{Jz}{N}\sum_{\vec{k}'} I^{\alpha\beta}_{\vec{k}',\vec{k}_1,(\vec{k}+\vec{k}_1-\vec{k}')\vec{k}} I^{\alpha\beta}_{\vec{k}\vec{k}',\vec{k}_1(\vec{k}+\vec{k}_1-\vec{k}')}$$

$$\times \frac{N(\bar{\Omega}_{\vec{k}'}) - N(\bar{\Omega}_{\vec{k}+\vec{k}_1-\vec{k}'})}{(\bar{\Omega}_{\vec{k}+\vec{k}_1-\vec{k}'} - \bar{\Omega}_{\vec{k}'}) + (\xi_l + \xi_{l_1} + \xi_{l_2})} \quad . \tag{69}$$

Note, as would be expected, that K vanishes at $T = 0\,^{\circ}\mathrm{K}$, and gives no correction to the zero-temperature spectrum.

It is rather apparent that, with these new corrections taken into account, one will no longer be able to obtain an exact solution for $\mathcal{G}^{(+)}(\xi_l)$ as was obtained in Sec. IV. However, we may obtain an approximate evaluation of $\mathcal{G}^{(+)}(\xi_l)$ using the variational principle[29] discussed in Appendix B. This variational principle assumes that $\tilde{I}^{\alpha\beta}_{\vec{k}\vec{k}_1,\vec{k}_1\vec{k}}(\xi_{l_1},\xi_{l_2})$ is symmetric[30] under the transformation $\xi_{l_1} \rightleftarrows \xi_{l_2}$ and $\vec{k} \rightleftarrows \vec{k}_1$. Referring to Eq. (69), we see that the first property above is correct. However, the second property ($\vec{k} \rightleftarrows \vec{k}_1$) is not quite correct due to the form of the I matrix elements. In this connection, we refer back to Eq. (59) which gives the lowest contribution to $\tilde{I}^{\alpha\beta}$. This expression contains an antisymmetric term[31] in $\vec{k}$ and $\vec{k}_1$. The antisymmetric term in this case rigorously gave no contribution to the cross section but it is not known whether this can be shown to be true in general. In any case, it can be shown for $\vec{k}$ and $\vec{k}_1$ near the zone edge ($u_{\vec{k}} \simeq u_{\vec{k}_1} \simeq 1$, $v_{\vec{k}} \simeq v_{\vec{k}_1} \simeq 0$) that $\tilde{I}^{\alpha\beta}_{\vec{k}\vec{k}_1,\vec{k}_1\vec{k}}(\xi_{l_1},\xi_{l_2})$ as given by Eqs. (68) and (69) is approximately symmetric under $\vec{k} \rightleftarrows \vec{k}_1$. With this approximation and a simple choice of a trial function, the variational principle of Appendix B yields the result

$$\mathcal{G}^{(+)}(\xi_l) \simeq \tfrac{4}{3} g(\vec{\epsilon}_i,\vec{\epsilon}_f) N S^2 B_3^2 \times \frac{L^{(2)}(\xi_l)}{1 - Jz\psi(\xi_l)/L^{(2)}(\xi_l)} , \tag{70}$$

where $L^{(2)}(\xi_l)$ is given by Eq. (63), and

$$\psi(\xi_l) = \frac{1}{N^2\beta^2}\sum_{\vec{k}\vec{k}_1}\sum_{l_1 l_2} f(\vec{k}) f(\vec{k}_1)(u_{\vec{k}}^2 + v_{\vec{k}}^2)(u_{\vec{k}_1}^2 + v_{\vec{k}_1}^2) \times D_{\vec{k}\alpha}(\xi_l + \xi_{l_1}) D_{\vec{k}\beta}(\xi_{l_1}) D_{\vec{k}_1\alpha}(\xi_l + \xi_{l_2}) D_{\vec{k}_1\beta}(\xi_{l_2}) \times \tilde{I}^{\alpha\beta}_{\vec{k}\vec{k}_1,\vec{k}_1\vec{k}}(\xi_{l_1},\xi_{l_2}) . \tag{71}$$

From Eq. (71) we see that any (assumed small) antisymmetric part of $\tilde{I}^{\alpha\beta}$ makes no contribution to ψ. Writing $\tilde{I}^{\alpha\beta}_{\vec{k}\vec{k}_1,\vec{k}_1\vec{k}} = I^{\alpha\beta}_{\vec{k}\vec{k}_1,\vec{k}_1\vec{k}} + K_{\vec{k}\vec{k}_1}(\xi_{l_1},\xi_{l_2})$, we then obtain

$$\mathcal{G}^{(+)}(\xi_l) = \tfrac{4}{3} g(\vec{\epsilon}_i,\vec{\epsilon}_f) N S^2 B_3^2 \left[\frac{L^{(2)}(\xi_l)}{1 - \frac{1}{2}J[L^{(2)}(\xi_l)L^{(2)}(\xi_l) + L^{(1)}(\xi_l)L^{(1)}(\xi_l)]/L^{(2)}(\xi_l) - Jz\psi'(\xi_l)/L^{(2)}(\xi_l)}\right] , \tag{72}$$

with

$$\psi'(\xi_l) = \frac{1}{N^2\beta^2}\sum_{\vec{k}\vec{k}_1}\sum_{l_1 l_2} f(\vec{k}) f(\vec{k}_1)(u_{\vec{k}}^2 + v_{\vec{k}}^2)(u_{\vec{k}_1}^2 + v_{\vec{k}_1}^2) D_{\vec{k}\alpha}(\xi_l + \xi_{l_1}) D_{\vec{k}\beta}(\xi_{l_1}) D_{\vec{k}_1\alpha}(\xi_l + \xi_{l_2}) D_{\vec{k}_1\beta}(\xi_{l_2}) K_{\vec{k}\vec{k}_1}(\xi_{l_1},\xi_{l_2}) . \tag{73}$$

Note that, in the absence of the higher-order vertex corrections obtained in $\psi'(\xi_l)$, Eq. (72) yields essentially the same result obtained previously [Eq. (62)], because $L^{(0)} \simeq L^{(1)} \simeq L^{(2)}$ due to the sharp peaking of the density-of-states function near the zone edge. This gives us some confidence that the variational method provides a reasonable approximation for treating the higher-order vertex corrections.

Unfortunately, a calculation of $\psi'(\xi_l)$, like that

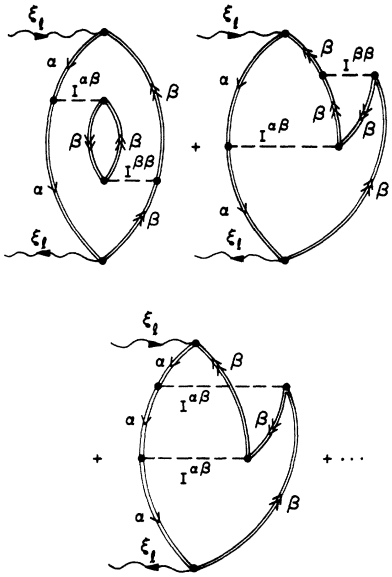

FIG. 9. Typical second-order irreducible vertex corrections leading to a modified vertex function $\Lambda_{\xi}(\xi_l, \xi_{l_1})$.

of the imaginary part of the second-order self-energy processes, is very complicated to carry out, and we can presently make no qualitative predictions about the effect of this term on the two-magnon Raman spectrum. Improved numerical calculations of the second-order self-energy for a zone-edge magnon, and calculations of the effects of the higher-order vertex corrections contained in $\psi'(\xi_l)$ are presently in progress, and results of these calculations are planned for a future publication.

VI. DISCUSSION

In this paper we have attempted to analyze the low-temperature behavior of two-magnon Raman spectra using a spin-wave approach based on the Dyson-Maleev formalism. We have found that, while the shift of the Raman peak to lower energies can be satisfactorily explained by the renormalization of the one-magnon energies in the Hartree-Fock approximation, the observed broadening of the spectra with increasing temperature appears to have a more complex origin. Preliminary crude calculations indicate that this broadening effect is probably not due to damping of one-magnon states, but more accurate calculations of the damping of a zone-edge magnon are needed to eliminate this possibility. We have also set up a formalism for treating the higher-order vertex corrections in the two-magnon Bethe-Salpeter equation, but the qualitative effect of these corrections is not yet known.

In conclusion, there exists the nagging possibility that the correct solution of this puzzle lies in contributions in the Hamiltonian or Raman tensor which we have ignored in this treatment. For example, in the Raman tensor we have discarded terms involving products of more than four magnon operators. At least in a graphical sense, certain of these higher-order contributions in the Raman tensor cannot be interpreted in terms of "two-magnon" scattering processes. Nevertheless such terms could be important for understanding the temperature dependence of the measured "two-magnon" cross section. These higher-order terms will be difficult to treat using the sort of spin-wave technique which we have employed in this paper. In the event that these processes become important with increasing temperature, it may indicate that a spin-wave approach is not the best way to tackle the problem. If this should be the case, some better method of decoupling the higher-order Green's functions in the spin-operator equation-of-motion method must be sought.

ACKNOWLEDGMENTS

We wish to thank Dr. J. Sólyom for sending us a copy of his paper prior to publication. We would also like to acknowledge several helpful discussions with Dr. C-Y. Young.

APPENDIX A

The three matrix elements which appear in Eq. (18) of Sec. II are

$$I^{\alpha\alpha}_{\vec{q}\vec{q}',\vec{p}\vec{p}'} = \gamma(p'-p)u_{\vec{q}}u_{\vec{q}'}v_{\vec{p}}v_{\vec{p}'} + \tfrac{1}{2}[\gamma(\vec{p})u_{\vec{q}}u_{\vec{q}'}v_{\vec{p}}u_{\vec{p}'} + \gamma(\vec{p}')v_{\vec{q}}v_{\vec{q}'}v_{\vec{p}}u_{\vec{p}'}], \tag{A1}$$

$$I^{\beta\beta}_{\vec{q}\vec{q}',\vec{p}\vec{p}'} = \gamma(\vec{q}'-\vec{q})u_{\vec{q}}u_{\vec{q}'}v_{\vec{p}}v_{\vec{p}'} + \tfrac{1}{2}[\gamma(\vec{q})u_{\vec{q}}v_{\vec{q}'}v_{\vec{p}}v_{\vec{p}'} + \gamma(\vec{q}')u_{\vec{q}}v_{\vec{q}'}u_{\vec{p}}u_{\vec{p}'}], \tag{A2}$$

$$I^{\alpha\beta}_{\vec{q}\vec{q}',\vec{p}\vec{p}'} = \gamma(\vec{p}'-\vec{p})u_{\vec{q}}u_{\vec{q}'}u_{\vec{p}}u_{\vec{p}'} + \gamma(\vec{q}'-\vec{q})v_{\vec{q}}v_{\vec{q}'}v_{\vec{p}}v_{\vec{p}'} + \gamma(\vec{q}-\vec{p}')v_{\vec{q}}u_{\vec{q}'}v_{\vec{p}}u_{\vec{p}'}$$
$$+\gamma(\vec{p}-\vec{q}')u_{\vec{q}}v_{\vec{q}'}u_{\vec{p}}v_{\vec{p}'} + \gamma(\vec{p})u_{\vec{q}}u_{\vec{q}'}u_{\vec{p}}v_{\vec{p}'} + \gamma(\vec{q})v_{\vec{q}}u_{\vec{q}'}v_{\vec{p}}v_{\vec{p}'} + \gamma(\vec{q}')v_{\vec{q}}u_{\vec{q}'}u_{\vec{p}}u_{\vec{p}'} + \gamma(\vec{p}')v_{\vec{q}}v_{\vec{q}'}u_{\vec{p}}v_{\vec{p}'}\,. \tag{A3}$$

Note that the order of the indices of the u's and v's in each term is the same as the order in which they occur in the I's.

In the Dyson-Maleev scheme employed in Ref. 18, one takes for the a sublattice spin operators the expressions given in Eq. (3). However, the

b sublattice spin operators are chosen according to

$$\tilde{S}^{+}_{j+\delta,b} = (2S)^{1/2} b^{\dagger}_{j+\delta}\left(1 - \frac{b^{\dagger}_{j+\delta} b_{j+\delta}}{2S}\right) ,$$

$$\tilde{S}_{j+\delta,b} = (2S)^{1/2} b_{j+\delta} , \tag{A4}$$

$$\tilde{S}^{z}_{j+\delta,b} = -S + b^{\dagger}_{j+\delta} b_{j+\delta} .$$

The corresponding matrix elements from this scheme are

$$I^{\alpha\alpha}_{\vec{q}\vec{q}',\vec{p}\vec{p}'} = I^{\beta\beta}_{\vec{q}\vec{q}',\vec{p}\vec{p}'}$$

$$= \gamma(\vec{p}'-\vec{p}) u_{\vec{q}} u_{\vec{q}'} v_{\vec{p}} v_{\vec{p}'} + \tfrac{1}{2}[\gamma(\vec{p}) u_{\vec{q}} u_{\vec{q}'} v_{\vec{p}} u_{\vec{p}'} + \gamma(\vec{q}) u_{\vec{q}} v_{\vec{q}'} v_{\vec{p}} v_{\vec{p}'}] , \tag{A5}$$

$$I^{\alpha\beta}_{\vec{q}\vec{q}',\vec{p}\vec{p}'} = \gamma(\vec{p}'-\vec{p}) u_{\vec{q}} u_{\vec{q}'} u_{\vec{p}} u_{\vec{p}'} + \gamma(\vec{q}'-\vec{q}) v_{\vec{q}} v_{\vec{q}'} v_{\vec{p}} v_{\vec{p}'} + \gamma(\vec{q}-\vec{p}') v_{\vec{q}} u_{\vec{q}'} v_{\vec{p}} u_{\vec{p}'}$$

$$+ \gamma(\vec{p}-\vec{q}') u_{\vec{q}} v_{\vec{q}'} u_{\vec{p}} v_{\vec{p}'} + \gamma(\vec{p}) u_{\vec{q}} u_{\vec{q}'} u_{\vec{p}} v_{\vec{p}'} + \gamma(\vec{q}) v_{\vec{q}} u_{\vec{q}'} v_{\vec{p}} v_{\vec{p}'} + \gamma(\vec{q}) u_{\vec{q}} v_{\vec{q}'} u_{\vec{p}} u_{\vec{p}'} + \gamma(\vec{p}) v_{\vec{q}} v_{\vec{q}'} v_{\vec{p}} u_{\vec{p}'} . \tag{A6}$$

Allowing for a difference in the way that Fourier transforms have been introduced, these results agree with the corresponding matrix elements given by Harris, *et al.*[18]

APPENDIX B

Here we discuss a variational principle for obtaining an approximate solution for the Raman cross section when higher-order vertex corrections are included in the two-magnon Bethe-Salpeter equation. In a compact notation, we can write the two basic equations [Eqs. (52) and (54)] of the present theory as

$$\tilde{\mathcal{G}}^{(+)}(q_0) = \sum_k V(k) \bar{D}(k;q_0) \Lambda(k;q_0) , \tag{B1}$$

$$\Lambda(k;q_0) = V(k) + Jz \sum_{k_1} \tilde{I}^{\alpha\beta}(k,k_1) \bar{D}(k_1;q_0) \Lambda(k_1;q_0) . \tag{B2}$$

Here $\tilde{\mathcal{G}}^{(+)} = \mathcal{G}^{(+)} / [\frac{4}{3} g(\vec{\epsilon}_i, \vec{\epsilon}_f) NS^2 B_3^2]$, and we have introduced some four-dimensional notation:

$$(\vec{k}, \xi_{l_1}) \to k , \qquad \frac{1}{N\beta} \sum_{\vec{k}} \sum_{l_1} \to \sum_k ,$$

$$(\vec{k}_1, \xi_{l_2}) \to k_1 , \qquad \frac{1}{N\beta} \sum_{\vec{k}_1} \sum_{l_2} \to \sum_{k_1} ,$$

$$q_0 = \xi_l , \qquad V(k) = f(\vec{k})(u^2_{\vec{k}} + v^2_{\vec{k}}) ,$$

$$\bar{D}(k;q_0) = D_{\vec{k}\alpha}(\xi_l + \xi_{l_1}) D_{\vec{k}\beta}(\xi_{l_1}) ,$$

and

$$\tilde{I}^{\alpha\beta}(k,k_1) = \tilde{I}^{\alpha\beta}_{\vec{k}\vec{k}_1,\vec{k}_1\vec{k}}(\xi_{l_1}, \xi_{l_2}) .$$

We assume that $\tilde{I}^{\alpha\beta}(k, k_1) = \tilde{I}^{\alpha\beta}(k_1, k)$ is symmetric in the discussion which follows.

Next we construct the following functional of Λ:

$$\tilde{\mathcal{G}}^{(+)}(\Lambda) = \sum_k 2V(k) \bar{D}(k;q_0) \Lambda(k;q_0)$$

$$- \sum_k \bar{D}(k;q_0) \Lambda(k;q_0)^2 + Jz \sum_{kk_1} \Lambda(k;q_0)$$

$$\times \bar{D}(k;q_0) \tilde{I}^{\alpha\beta}(k,k_1) \bar{D}(k_1;q_0) \Lambda(k_1;q_0) , \tag{B3}$$

where we treat Λ as an arbitrary function of k. By taking the variational derivative of Eq. (B3), it is straightforward to show that the above functional is stationary with respect to variations in Λ, when Λ satisfies Eq. (B2). Furthermore the stationary value of the functional is exactly $\mathcal{G}^{(+)}(q_0)$ as given by Eq. (B1).

We apply the variational principle by choosing the simplest trial function we can think of:

$$\Lambda(k;q_0) = AV(k) , \tag{B4}$$

where $A = A(q_0)$ is a constant (independent of k). Inserting this into the functional form Eq. (B3), and requiring the functional to be stationary with respect to variation of A yields

$$A = \left(1 - Jz \sum_{kk_1} V(k) V(k_1) \bar{D}(k;q_0) \bar{D}(k_1;q_0) \tilde{I}^{\alpha\beta}(k,k_1) / \sum_k V(k)^2 \bar{D}(k;q_0)\right)^{-1} . \tag{B5}$$

The resulting stationary value of the functional is then found to be

$$\tilde{\mathcal{G}}^{(+)}(q_0) = A \sum_k V(k)^2 \bar{D}(k;q_0) . \tag{B6}$$

Writing out these results explicitly then yields Eq. (70) of Sec. V.

As discussed in Sec. V, in the case where the higher-order vertex corrections in $\tilde{I}^{\alpha\beta}$ may be ignored (e.g., at zero temperature), the simple choice of a trial function given by Eq. (B4) yields a very good approximation for $\tilde{\mathcal{G}}^{(+)}(\xi_l)$. This is not surprising because the exact solution of the simple "ladder" approximation Bethe-Salpeter equation is of the form

$$\Lambda_{\vec{k}}(\xi_l, \xi_{l_1}) = \Lambda_{\vec{k}}(\xi_l) = f(\vec{k})[A(\xi_l)(u^2_{\vec{k}} + v^2_{\vec{k}}) + B(\xi_l)] , \tag{B7}$$

where A and B are constants (independent of $\vec{k}$).

If Eq. (B7) is substituted into the functional form Eq. (B3), and the functional is made stationary with respect to variation of A and B, it is straightforward to verify that the variational principle then generates the exact solution for $\tilde{\mathcal{G}}^{(+)}(\xi_l)$ as given by Eq. (62).

---

*Work sponsored by the Department of the Air Force.

[1]P. A. Fleury, S. P. S. Porto, L. E. Cheesman, and H. J. Guggenheim, Phys. Rev. Letters 17, 84 (1966); P. A. Fleury and S. P. S. Porto, J. Appl. Phys. 39, 1035 (1968); P. A. Fleury and R. Loudon, Phys. Rev. 166, 514 (1968).

[2]P. A. Fleury, Phys. Rev. Letters 21, 151 (1968).

[3]Yu. A. Popkov, V. I. Fomin, and B. V. Beznosikov, Zh. Eksperim. Teor. Fiz. Pis'ma v Redaktsiyu 11, 394 (1970) [Sov. Phys. JETP Letters 11, 264 (1970)].

[4]S. R. Chinn, H. J. Zeiger, and J. R. O'Connor, J. Appl. Phys. 41, 894 (1970); Phys. Rev. B 3, 1709 (1971).

[5]S. R. Chinn, Phys. Rev. B 3, 121 (1971).

[6]P. A. Fleury, Phys. Rev. 180, 591 (1969).

[7]S. R. Chinn and H. J. Zeiger, Phys. Rev. Letters 21, 1589 (1968).

[8]P. A. Fleury, J. M. Worlock, and H. J. Guggenheim, Phys. Rev. 185, 738 (1969).

[9]T. Moriya, J. Phys. Soc. Japan 23, 490 (1967); J. Appl. Phys. 39, 1042 (1968).

[10]R. J. Elliott, M. F. Thorpe, G. F. Imbusch, R. Loudon, and J. B. Parkinson, Phys. Rev. Letters 21, 147 (1968).

[11]R. J. Elliott and M. F. Thorpe, J. Phys. C 2, 1630 (1969).

[12]T. Kawasaki, J. Phys. Soc. Japan 29, 1144 (1970).

[13]J. Sólyom (unpublished).

[14]V. G. Vaks, A. I. Larkin, and S. A. Pikin, Zh. Eksperim. i Teor. Fiz. 53, 281 (1967) [Sov. Phys. JETP 26, 188 (1968)].

[15]E. M. Pikalev, M. A. Savchenko, and J. Sólyom, Zh. Eksperim. i Teor. Fiz. 55, 1404 (1968) [Sov. Phys. JETP 28, 734 (1969)].

[16]D. C. Herbert, J. Math. Phys. 10, 2255 (1969).

[17]D. C. Herbert, J. Phys. C 3, 891 (1970).

[18]A. B. Harris, D. Kumar, B. I. Halperin, and P. C. Hohenberg, Phys. Rev. B 3, 961 (1971).

[19]This is the scheme used in Ref. 18. A clear discussion of the various correspondences has been given by Dembinski [S. T. Dembinski, Physica 30, 1217 (1964)].

[20]The three-body term does not occur if one applies the Dyson correspondence on sublattice a and the conjugate Dyson correspondence on sublattice b. However, we have checked that none of the *explicit* results presented in this paper are affected if one uses this alternative approach.

[21]T. Oguchi, Phys. Rev. 117, 117 (1960).

[22]F. J. Dyson, Phys. Rev. 102, 1217 (1956).

[23]See, e. g., A. A. Abrikosov, L. P. Gorkov, and I. E. Dzyaloshinski, *Methods of Quantum Field Theory in Statistical Physics* (Prentice-Hall, Englewood Cliffs, N. J., 1963).

[24]M. Bloch, Phys. Rev. Letters 9, 286 (1962).

[25]M. Bloch, J. Appl. Phys. 34, 1151 (1963).

[26]See, e. g., Ref. 15. The well-known intuitive or heuristic method of Keffer and Loudon leads to the same result for cubic structures [F. Keffer and R. Loudon, J. Appl. Phys. 32, 25 (1961)].

[27]G. S. Rushbrooke and P. J. Wood, Mol. Phys. 1, 257 (1958); 6, 409 (1963).

[28]M. E. Lines, Phys. Rev. 164, 736 (1967); 135, A1336 (1964); 139, A1304 (1965).

[29]For a discussion of the application of analogous variational principles to other transport problems, see, e.g., A. K. Rajagopal, Phys. Rev. 142, 152 (1966); R. W. Davies, *ibid.* 162, 621 (1967); D. C. Langreth, *ibid.* 181, 753 (1969).

[30]Note that $\tilde{I}^{\alpha\beta}$ is also a function of $\xi_l \to \hbar\omega + 10^+$ through the last term in Eq. (69). We have suppressed this dependence for notational simplicity.

[31]The antisymmetric term does not appear if one uses the alternative Dyson-conjugate Dyson scheme. This may indicate that the alternative scheme is a somewhat more symmetric way of applying the Dyson-Maleev transformation, i.e., within the sort of approximation scheme we are using.